INTERNATIONAL ATOMIC ENERGY AGENCY
UNITED NATIONS EDUCATIONAL, SCIENTIFIC AND CULTURAL ORGANIZATION

INTERNATIONAL CENTRE FOR THEORETICAL PHYSICS
34100 TRIESTE (ITALY) - P.O.B. 586 - MIRAMARE - STRADA COSTIERA 11 - TELEPHONE: 2240-1
CABLE: CENTRATOM - TELEX 460892-1

SMR/388 - 39

SPRING COLLEGE IN MATERIALS SCIENCE
ON
'CERAMICS AND COMPOSITE MATERIALS'
(17 April - 26 May 1989)

A STRONG-COUPLING MECHANISM IN THE HIGH-T_c COPPER OXIDES

J.B. GOODENOUGH
University of Texas At Austin
Center For Materials Science and Engineering - Etc. 5.160
Austin Texas 78712
U.S.A.

appear: Proceedings MRS meeting in San Diego, Calif, April 21-28, 1988

IDENTIFYING THE PAIRING MECHANISM IN HIGH-T_c SUPERCONDUCTORS

J.B. Goodenough, A. Manthiram, and J. Zhou
Center for Materials Science & Engineering, ETC 5.160
University of Texas at Austin, Austin, TX 78712-1084

ABSTRACT

It is argued that the origin of the high transition temperatures observed in $Ba_{1-x}K_xBiO_3$ and the copper-oxide superconductors with perovskite-related structures is due to two factors: (1) overlap of a partially filled σ^* band of primarily cation character and a π or π^* band of mostly O-2p_π parentage permits charge transfer between cation and anion subarrays with oxygen-atom displacement perpendicular to a M-O-M bond axis and (2) bondlength mismatch places the M-O-M bondlength under a compressive or tensile stress. Relief of a compressive stress by the bending of a M-O-M bond from 180° introduces a strong electron-lattice interaction with holes; a 180° Cu-O-Cu bond allows strong electron-lattice coupling with electrons of a $Cu^{2+/+}$ redox couple, but not with holes in a $Cu^{3+/2+}$ redox couple.

INTRODUCTION

A superconductor is a normal metal above its transition temperature T_c; at temperatures $T < T_c$, a condensation of electron pairs is stabilized by the opening up of an energy gap 2Δ in the density of electron states at the Fermi energy E_F. Any alternate mechanism for opening up an energy gap E_g at E_F in the Hartree-Fock one-electron states, which would yield a normal semiconductor, is competitive with superconductivity.

Two cooperative phenomena that open up an energy gap E_g at E_F and thus compete with superconductivity are the formation of a charge-density wave (CDW) -- or a spin-density wave (SDW) -- and the correlation splitting (CS) associated with localized atomic magnetic moments [1]. The oxide system $Ba_{1-x}K_xBiO_3$ represents a competition between CDW formation and superconductivity; the high-T_c copper-oxide systems all represent a competition between CS and superconductivity.

The condensation of superconductive electron-pair states requires the existence of a coupling energy between the paired electrons that is greater than their coulomb repulsion. In conventional superconductors, Cooper pairs are formed by electron-phonon interactions. However, this pairing mechanism gives an upper limit to T_c near $T_c = 40$ K; therefore, the observation of a T_c as high as 120 K has forced consideration of alternate mechanisms. Three basic approaches have been formulated: (1) a new type of electronic state: e.g. the resonating-valence bond (RVB) [2], (2) an electron-electron interaction to replace the conventional electron-phonon interaction; e.g. atomic polarization [3], excitons [4], magnetic bags [5], or spin-spin interactions between itinerant and localized electrons [6], and (3) strong electron-lattice interactions -- probably enhanced by a high electronic polarizability -- that may give rise to the condensation of large polarons visualizable in real space [7]. In order to distinguish between these three approaches, it is necessary to inquire into two aspects of the high-T_c oxide superconductors: their distinguishing electron configurations near E_F and any unique structural features that could introduce unusual electron-lattice coupling.

THE SYSTEM $Ba_{1-x}K_xBiO_3$

The compound $BaBiO_3$ has a structure derived from the cubic perovskite structure, Fig. 1. In this ABO_3 structure, the tolerance factor

$$t = (r_A + r_O)/\sqrt{2}(r_B + r_O) \qquad (1)$$

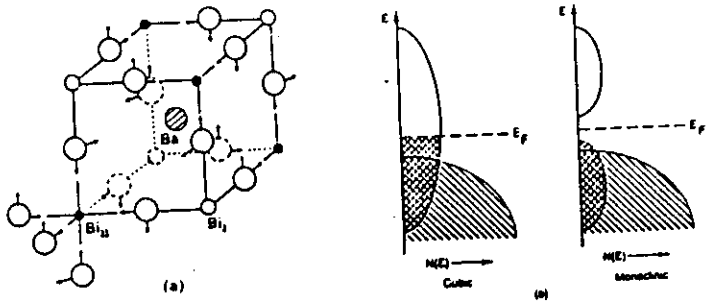

Fig. 1 (a) The cubic perovskite structure of high-temperature $BaBiO_3$ and, arrows, the direction of the oxygen-atom displacements on transforming to the monoclinic structure. (b) The energy density N(E) of one-electron states near E_F for (i) cubic and (ii) monoclinic $BaBiO_3$.

which relates the A-O and B-O bond lengths, represents ideal bondlength matching for $t = 1$. Since the A-O and B-O bonds have different thermal-expansion coefficients, t increases with increasing temperature; therefore the condition $t = 1$ can, at best, only be satisfied at one temperature. A $t = 1$ at the formation temperature results in a $t < 1$ at lower temperatures. A $t < 1$ places the B-O bonds under compression, the A-O bonds under tension. This incompatibility can be relieved by a cooperative rotation of the BO_6 octahedra that bends the B-O-B bond. In $BaBiO_3$, such a cooperative rotation about a [110] axis represents only one component of the oxygen-atom displacements. The second component shown in Fig. 1 is due to the formation of a "negative U" CDW.

In an octahedral site of oxide ions, covalent mixing between Bi-6s and O-2p_σ orbitals makes small (< 2 eV) any intraatomic CS between the $6s^1$ and $6s^2$ energy levels at Bi^{4+} and Bi^{3+} ions and it introduces a significant 180° Bi-O-Bi interatomic interaction. In this situation, a bandwidth $W > U$, where U is the CS, suppresses the formation of any bismuth magnetic moment in the absence of an applied magnetic field; however, the bandwidth is narrow enough to sustain the formation of a CDW. As shown in Fig. 1, oxygen displacements toward Bi_{II} atoms and away from Bi_I atoms introduces distinguishable Bi subarrays and a charge transfer represented formally by

$$2Bi^{4+} \rightarrow Bi_I^{(4-\delta)+} + Bi_{II}^{(4+\delta)+} \qquad (2)$$

A $\delta = 1$ would correspond to the chemical disproportionation of Bi^{4+} into Bi_I^{3+} and Bi_{II}^{5+}; in fact, a smaller $\delta = 0.5$ occurs [8]. The resulting change in translational symmetry introduces a splitting of the σ^* band of primarily Bi-6s parentage, and monoclinic $BaBiO_3$ is a diamagnetic semiconductor.

The CDW has its maximum stability where a band is half-filled [1]. Shifting of E_F either up or down by reduction or oxidation of the BiO_3 array requires a change in the wavelength of the CDW with subsequent lowering of its stability and hence of the transition temperature T_t below which it is formed. Although a single-band picture would be symmetric with respect to reduction vs oxidation, it is apparent from Fig. 1(b) that this symmetry may not be applicable to $BaBiO_3$ because of the overlap of the σ^* and π bands.

Substitution of K for Ba in $Ba_{1-x}K_xBiO_3$ oxidizes the BiO_3 array, which lowers E_F into the lower σ^* band and/or the π band. A tentative phase diagram for the system [9,10] shows that the commensurate CDW associated with the monoclinic structure of low-temperature $BaBiO_3$ gives way to a more complex CDW in the compositional interval

$0.1 < x < 0.25$; complete suppression of the CDW in the interval $0.3 < x < 0.5$ gives a cubic superconductor with a T_c as high as 30 K at smaller x. This phase appears to be described as a Bardeen-Cooper-Schrieffer (BCS) superconductor with weak to moderate electron-phonon coupling.

The cubic phase is characterized by a large-amplitude oxygen vibration perpendicular to the Bi-O-Bi bond axis [11]. Oxygen displacements perpendicular to the bond axis introduce (or enhance) a π component into the conduction-band states at E_F, which would stabilize electrons at neighboring Bi atoms. Thus the large-amplitude oxygen vibrations would couple strongly to conduction electrons because the overlap of σ^* and π bands makes polarization fluctuations sensitive to the oxygen displacements.

THE SYSTEM $La_{2-x}Sr_xCuO_4$

Where W = U occurs at a bandwidth W that is too great for CDW formation, a half-filled band having W < U is split in two by the correlation splitting CS [1]. A CS has its maximum stability where the conduction band is half-filled; the atoms associated with the half-filled band are all single-valent.

The introduction of either electrons into the upper Hubbard band or holes into the lower Hubbard band creates a mixed-valent situation; the charge carriers thus created may move diffusively as small polarons, as itinerant charge carriers without any activation energy in the mobility, or by variable-range hopping from one dopant center to another. Small polarons do not give rise to a well-defined Fermi surface and hence do not condense out as superconductive pairs. The mobile charge carriers are transformed from small polarons to itinerant carriers as the bandwidth increases to the value W = U where the bandgap E_g due to CS disappears. Moreover, the introduction of charge carriers into either the upper or lower Hubbard band reduces U. Therefore doping an antiferromagnetic semiconductor (W < U) having a W only a little smaller than U for a half-filled band may lower U to where the condition W > U applies. As W exceeds U with increased doping, the Néel temperature T_N below which long-range antiferromagnetic ordering occurs must decrease; the atomic magnetic moment also decreases, but a CS and reduced atomic magnetic moments may persist into a phase exhibiting only short-range magnetic order.

This situation appears to be illustrated by the system $La_{2-x}Sr_xCuO_4$; but as in the case of $Ba_{1-x}K_xBiO_3$, the band symmetry is removed by an overlap of the σ^*_{x2-y2} conduction band and a π^* band of primarily O-$2p_\pi$ parentage, see below.

Fig. 2 illustrates the high-temperature tetragonal structure of the antiferromagnetic semiconductor La_2CuO_4. The tolerance factor t relating the La-O and Cu-O bondlengths is identical to that of the perovskite structure, equation (1), and a thermal-expansion mismatch makes (1-t) increase with decreasing temperature. The resulting compressive stress on the Cu-O bonds is relieved by a cooperative tilting of the elongated CuO_6 octahedra around a [110] axis, which reduces the symmetry from tetragonal to orthorhombic at lower temperature.

Band-structure calculations for La_2CuO_4 give a Fermi energy E_F lying in a broad σ^* band just above the top of a π^* band [12,13]. However, the observation of antiferromagnetic order with a copper magnetic moment $\mu_{Cu} \approx 0.5\ \mu_B$ [14] indicates that the band-structure calculation must be amended by the introduction of a CS of the σ^* band, Fig. 3(a). Moreover, observation of a μ_{Cu} demonstrates that the top of the σ^* band is primarily of Cu-3d parentage, and a large tetragonal (c/a > 1) distortion of the CuO_6 octahedra makes the assignment primarily Cu-$3d_{x2-y2}$ parentage. A σ^*_{x2-y2} band containing one hole per Cu atom is just half-filled, and the reduction of μ_{Cu} from 1 μ_B indicates that W < U approaches W = U.

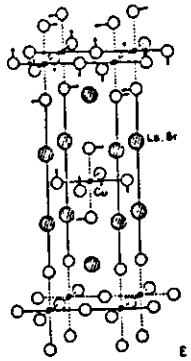

Fig. 2 The tetragonal (T) K_2NiF_4 structure of high-temperature La_2CuO_4. Arrows indicate directions of oxygen-atom displacements on transforming to the orthorhombic phase.

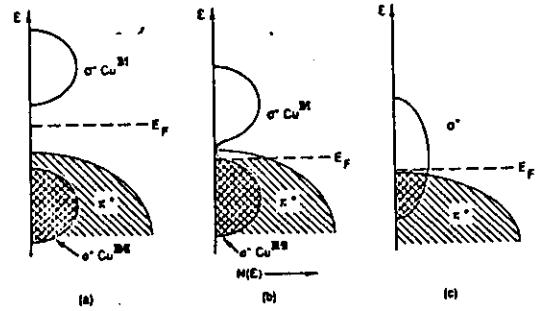

Fig. 3 Schematic energy density N(E) of one-electron states for $La_{2-x}Sr_xCuO_4$: (a) x = 0, (b) x = 0.15, (c) x = 0.4.

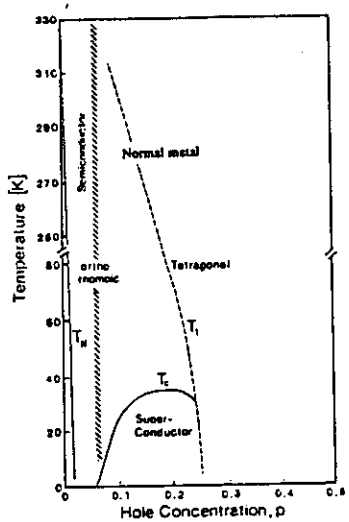

Fig. 4 Tentative phase diagram for $La_{2-x}Sr_xCuO_4$.

Substitution of Sr^{2+} for La^{3+} oxidizes the CuO_2 layers and yields the tentative phase diagram shown in Fig. 4 provided a high pressure of oxygen is used for $x > 0.15$ to retain full oxygen stoichiometry [15]. We address three questions:

- How does $\mu_{Cu} \approx 0.5\ \mu_B$ in La_2CuO_4 change on crossing the transition from an antiferromagnetic semiconductor to a superconductor?
- Where are the mobile holes that condense into superconductive pairs?
- Can we identify an unusual electron-lattice coupling?

In order to investigate the first question, we prepared $La_2CuO_{4+\delta}$ at 23 kbar and 800 °C in a double high-pressure cell containing CrO_3 on one side and La_2CuO_4 on the other of a stabilized-zirconia disc permeable to oxygen [16]. Decomposition of CrO_3 to Cr_2O_3 and O_2 creates a high oxygen pressure on the sample. Introduction of interstitial oxygen oxidizes the sample, and it becomes a superconductor ($T_c \approx 30$ K). The intersitital oxygen enters sites between two LaO layers that are coordinated by four La and four O atoms [17]. We had predicted that the interstitial oxygen would be present in this site as O^{2-}, a prediction born out for the interstitial oxygen in $La_2NiO_{4.13}$ [18]. However, in $La_2CuO_{4.03}$ cooled rapidly enough to lowest temperatures that phase separation below room temperature -- observed in polycrystalline samples [19] -- did not occur, the interstitial oxygen forms a complex cluster with two of the four neighboring oxygen atoms [17]. From the O-O distances of the cluster, it might be argued that one hole per intersitial oxygen is trapped at the interstitial oxygen. However, trapping of one hole at an oxygen cluster centered at the interstitial oxygen does not reconcile the discrepancy in the value of $\delta \approx 0.05$ determined by iodometric titration and $\delta \approx 0.14$ by thermogravimetric analysis (TGA) [16]. A similar discrepancy was reported for samples prepared at lower oxygen pressures [20]. We interpreted the discrepancy to indicate $\delta \approx 0.05$ interstitial O^{2-} ions in the bulk and ca. 0.1 superficial oxygen introduced at high pressure. In either case, the observed T_c is consistent with the introduction of about 0.1 holes per Cu atom in the CuO_2 sheets.

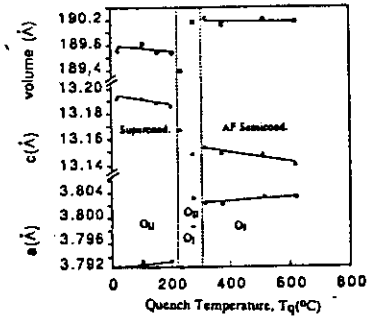

Fig. 5 Variation of room-temperature volume and lattice parameters with quench temperature T_q for $La_2CuO_{4+\delta}$ heated successively to higher T_q.

Whatever the exact character of the interstitial oxygen, the TGA curve shows an abrupt loss of oxygen in the interval $225 < T < 275$ °C [16]. Fig. 5 gives the variation in room-temperature lattice parameter with quench temperature T_q for a high-oxygen-pressure sample raised successively to higher T_q in air before quenching to room temperature for X-ray diffraction. A first-order phase change occurs in the interval $225 < T_q < 275$ °C, which yielded two phases: the low-temperature superconductor and the high-temperature antiferromagnetic semiconductor. A small increase in volume with loss of interstitial oxygen results from a remarkable increase in 1/2(a+b). The increase in Cu-O bondlength on going to the antiferromagnetic phase is even more pronounced as the Cu-O-Cu bond angle becomes more removed from 180°. This finding demonstrates that shortening of the Cu-O bond in the CuO_2 sheets on oxidation is consistent with an important suppression of μ_{Cu} as $W < U$ becomes $W > U$. An expansion of the Cu-O bondlength on passing from the

superconductive to the antiferromagnetic phase is characteristic of all the copper-oxide superconductors [21].

Independent magnetic [22] and neutron-scattering [23] measurements indicate that the presence of a μ_{Cu}, though reduced, persists into the superconductive compositional range of $La_{2-x}Sr_xCuO_4$. However, there is no indication that the existence of a μ_{Cu} enhances the superconductive T_c. What is remarkable is the fact that it does not suppress the superconductivity. This observation leads inexorably to the question of the location of the mobile holes responsible for the superconductivity.

The most definitive answer to this questions comes from electron spectroscopy [24-27]. It places the holes in states that are predominantly of O-$2p_\pi$ character lying in the CuO_2 sheets. We have argued elsewhere [28] that the Madelung stabilization of the O-2p states just balances the ionization energy required to remove one electron from a Cu^{2+} ion to an O^- ion. This balance causes the $Cu^{3+/2+}$ redox energy to be overlapped by the O-2p energies, and covalent mixing between Cu$3d_{xy}$ and O-$2p_\pi$ orbitals can result in a π^* band that is primarily O-$2p_\pi$ in character while mixing of Cu-$3d_{x2-y2}$ and O-$2p_\sigma$ orbitals results in a σ^* band that is primarily Cu-$3d_{x2-y2}$ in character. Moreover, so long as a μ_{Cu} persists, there is a correlation splitting of the σ^* band that places the top of the π^* band above the top of the lower σ^* band as illustrated in Fig. 3(b). As a consequence, the role of a residual μ_{Cu} in the superconductive phase appears to be the maintenance of a CS of the σ^* band, which results in mobile holes in π^* bands of primarily O-$2p_\pi$ character. These holes can give rise to superconductivity, but holes in a correlation-split σ^* band would not.

Demonstration of this latter assertion comes from the suppression of T_c for $x > 0.25$. With the total disappearance of μ_{Cu} with increasing x, the correlation splitting vanishes; in this case, holes would be more stable in σ^* -band states, which are the more strongly antibonding, so the Cu-O-Cu bond angle would straighten out to 180°, which would remove the mixed symmetry. Such a straightening results in an orthorhombic-to-tetragonal transition, and superconductivity vanishes in the tetragonal phase. There remains some controversy in the literature over whether the superconductivity-to-normal metal transition coincides with the orthorhombic-to-tetragonal transition; the experimental situation may be confused by the possibility of introducing excess oxygen in a portion of the sample under the preparative conditions used to supply a high partial pressure of oxygen.

This analysis leads to two predictions: movement of E_F from the π^* band into the σ^* band as shown in Fig. 3(c) would result in (i) a transition from p-type to n-type conductivity in the normal metal and (ii) a transition from a Cu-2p spectrum characteristic of Cu^{2+} to one characteristic of Cu^{3+} as found in $NaCuO_2$ [29]. Preliminary measurements appear to confirm both of these predictions [30].

Finally, the possibility of a strong interaction between the conduction electrons and the transverse optical-mode oxygen vibrations perpendicular to a Cu-O-Cu bond axis has already been pointed out. If the CuO_2 plane is under compression, this interaction is strong where the Cu-O-Cu bond angle is bent from 180° and the charge carriers are holes; a hole stabilizes a straightening of the bond angle, and the relatively slow response of the oxygen displacement provides time to attract a second hole. The mechanism represents a strong electron-phonon interaction that is enhanced by the polarizability of the conduction-electron charge density resulting from an overlap of the σ^* and π^* bands. In this strong-coupling limit, the Cooper pairs become condensed into a volume of sufficiently small coherence length ($\xi \sim 10$ Å) that the distinction between a Cooper pair and a large bipolaron may become blurred.

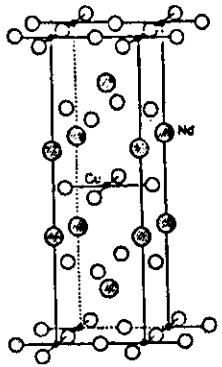

Fig. 6 The tetragonal (T) structure of Nd_2CuO_4.

Conversely, if the CuO_2 plane is under tension, the Cu-O-Cu bond angle is 180° and the electron-lattice interaction is strong where the charge carriers are electrons of the $Cu^{2+/+}$ couple; in this case an electron stabilizes a bending of the Cu-O-Cu bond angle, and the relatively slow response of the oxygen displacement provides time to attract a second electron. This situation is realized in the tetragonal T' structure of Nd_2CuO_4, Fig. 6[31], where the smaller Nd^{3+} ion -- relative to La^{3+} -- creates so small a tolerance factor t that the c-axis oxygen of the tetragonal T phase of high-temperature La_2CuO_4, Fig. 2, are displaced to the plane of tetrahedral sites of the Nd bilayer. This displacement expands the a-axis, thereby removing the compression of the Cu-O bonds of a CuO_2 plane. Doping this phase p-type by Sr substitution for Nd leaves the system semiconducting [32]; but doping it n-type by, for example, Ce substitution for Nd leads to a superconductive phase in a narrow compositional range [33]. According to the model of electron-lattice coupling we are proposing, n-type superconductivity requires sufficient electron doping to make W > U and thus suppress μ_{Cu}, but insufficient doping to destroy the phase.

SYSTEMS WITH THE $YBa_2Cu_3O_{6+x}$ STRUCTURE

Extension of the ideas presented above to the other high-T_c copper oxides is straightforward. In every case there is an interface between a CuO_2 layer and an MO layer that is subject to the tolerance-factor constraint of equation (1). Moreover, they are p-type conductors in their normal state with a Cu-O-Cu angle bent from 180° in their superconductive state. However, in the phases with multiple CuO_2 sheets separated by Y^{3+} and/or Ca^{2+} ions, the bending of the Cu-O-Cu bond angle from 180° is induced by the symmetry of the structure; the magnitude of the bending merely adjusts to relieve any stresses introduced by a t ≠ 1. In this case, a larger concentration of holes may be introduced into the CuO_2 sheets before the Cu-O-Cu bond angle is straightened out to 180°. Since T_c appears to vary with the concentration of mobile holes in the CuO_2 sheets [34-36], at least for smaller E_{VB}-E_F, the maintenance of a bent Cu-O-Cu bond angle to higher hole concentrations allows the realization of a higher value of T_c.

In view of this situation, it is relevant to review briefly the evidence for π^*-band holes in the $YBa_2Cu_3O_{6+x}$ structure and for a T_c varying with the π^* -band hole concentration.

Placement of the mobile holes responsible for superconductivity into π^* -band states of the $Cu(2)O_2$ sheets that are primarily of O-$2p_\pi$ character comes from XPS evidence for a trapping out of mobile holes at oxygen-atom clusters centered at a-axis oxygen in the $Cu(1)O_x$ planes of $YBa_{2-y}La_yCu_3O_{6+x}$ [26]. A trapping out of mobile holes in the $Cu(1)O_x$ layers for x > 1 was verified independently by Hall measurements on the system $Nd_{1+y}Ba_{2-y}Cu_3O_{6+x}$ [35]. We have also shown that, by co-doping with Ca and La in the system $Y_{1-z}Ca_zBa_{2-y}La_yCu_3O_{6+x}$, it is possible to change the magnitude of the internal electric field

parallel to the c-axis so as to suppress hole trapping at disordered oxygen in the $Cu(1)O_x$ planes [38]. As is illustrated in Fig. 7, a T_c > 80 K is maintained in samples annealed in O_2 at 400 °C followed by slow cooling to 250 °C, provided there is no hole trapping; T_c decreases essentially lineraly with x above a critical oxygen concentration x_c that increases with Ca concentration z. The figure also illustrates that T_c is independent of the orthorhombic-tetragonal phase transition associated with oxygen ordering in the $Cu(1)O_x$ plane, an observation that is consistent with the hypothesis that the Cu-O-Cu bond angle is the critical structural feature for high-T_c superconductivity. Attempts to correlate a fall-off in T_c with total oxidation state cannot be valid; what would be valid is any correlation with the concentration of mobile holes in the CuO_2 sheets and the Cu-O-Cu bond angle in these sheets. The interesting data of Tokura et al [39] should be reconsidered from this perspective.

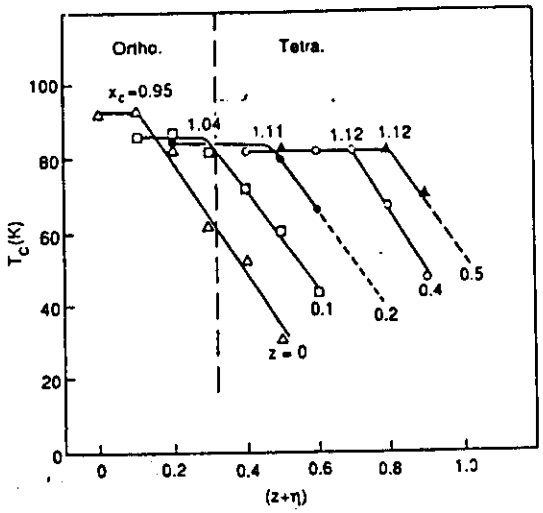

Fig. 7 Variation of T_c with y = z + η for various values of z in the system $Y_{1-z}Ca_zBa_{2-y}La_yCu_3O_{6+x}$ annealed in air at 400 °C.

In order to perform a correlation of the latter type, it is necessary to be aware of the complex hole transfer that occurs between $Cu(1)O_x$ planes and $Cu(2)O_2$ sheets. In addition to the possibility of hole trapping at disordered oxygen in the Cu(1)Ox planes, there is also the problem of hole trapping at Cu(1) atoms oxidized from Cu^+ to Cu^{2+}. The $YBa_2Cu_3O_{6+x}$ phase diagram provides evidence that, in the ordered structures, holes are transferred to the $Cu(2)O_2$ sheets once the Cu(1) atoms neighboring an oxygen in the $Cu(1)O_x$ plane are oxidized to Cu^{2+} [40]. The phase diagram exhibits a step in T_c vs x near x = 0.67. Electron microscopy has established the appearance of interchain ordering at x = 0.5; with perfect ordering, half of the Cu(1) atoms would remain Cu^{1+} ions coordinated to only two c-axis oxygen, so 0.125 holes per Cu(2) atom would be transferred to the $Cu(2)O_2$ sheets. Further oxidation of the $Cu(1)O_x$ planes would convert the remaining Cu(1) from Cu^+ to Cu^{2+} ions in the interval 0.5 < x < 0.75 before additional holes were transferred to the $Cu(2)O_2$ sheets. Long-range intrachain and interchain ordering within an untwinned grain of an x = 0.75 sample has now been observed [41]. However, the realization of perfect long-range order is never achieved uniformly over a bulk sample, so the step in T_c vs x due to oxidation of Cu(1) from Cu^+ to Cu^{2+} covers a narrower compositional range than 0.5 < x < 0.75 and is not flat as would be expected for a two-phase compositional range.

Support of this work by the Robert A. Welch Foundation, Houston, Texas and the Texas Advanced Research Program, Proposal #4257 is gratefully acknowledged.

REFERENCES

1. J.B. Goodenough, Progress in Solid State Chem. 5, 145 (1971).
2. P.W. Anderson, Science 235, 1196 (1987).
3. W.A. Little, Phys. Rev. 134, A1416 (1964).
4. V.L. Ginzburg, Zh. Esp. Teor, Fiz. 47, 2318 (1964).
5. J.R. Schrieffer, X.G. Wen, and S.-C. Zhang, Phys. Rev. Lett 60, 944 (1988).
6. V.J. Emery, Phys. Rev. Lett 58, 2797 (1987).
7. A.S. Alexandrov, J. Ranninger, and S. Robaszkiewicz, Phys. Rev. B33, 4526 (1986).
8. C. Chaillout, A. Santoro, J.P. Remeika, A.S. Cooper, G.P. Espinosa, and M. Marezio, Solid State Comm. 65, 1363 (1988).
9. R.J. Cava, B. Batlogg, J.J. Krajewski, R. Farrow, L.W. Rupp, Jr., A.E. White, K. Short, W.F. Peck, and T. Kometani, Nature 332, 814 (1988).
10. D.G. Hinks, B. Dabrowski, J.D. Jorgensen, A.W. Mitchell, D. R. Richards, Shiyou Pei, and Donglu Shi, Nature 333, 836 (1988).
11. J.P. Wignacourt, J.S. Swinnea, H. Steinfink, and J.B. Goodenough, Appl. Phys. Lett. 53, 18 (1988).
12. L.F. Mattheiss, Phys. Rev. Lett. 58, 1028 (1987).
13. J. Yu, A.J. Freeman, and J.H. Xu, Phys. Rev. Lett. 58, 1035 (1987).
14. D. Vaknin, S.K. Sinha, D.E. Moncton, D.C. Johnston, J.M. Newsam, C.R. Safinya, and M.E. King, Jr., Phys. Rev. Lett. 58, 2802 (1987).
15. J.B. Torrance, Y. Tokura, A.J. Nazzal, A. Bezinge, T.C. Huang, and S.S.P. Parkin, Phys. Rev. Lett. 61, 1127 (1988).
16. J. Zhou, S. Sinha, and J.B. Goodenough, Phys. Rev. B (in press).
17. C. Chaillout, S.W. Cheong, Z. Fisk, M.S. Lehmann, M. Marezio, B. Morosin, and J.E. Schirber, Physica C (submitted).
18. J.D. Jorgensen, B. Dabrowski, S. Pei, D.R. Richards, and D.G. Hinks, Phys. Rev. B (submitted).
19. J.D. Jorgensen, B. Dabrowski, Shiyou Pei, D.G. Hinks, L. Soderholm. B. Morosin, J.E. Schirber, E.L. Venturini, and D.S. Ginley, Phys. Rev. B38, 11337 (1988).
20. J.E. Schirber, B. Morosin, R.M. Merill, P.F. Hlava, E.L. Venturini, J.F. Kwak, P.J. Nigrey, R.J. Baughman, and D.S. Ginley, Physica C 152, 121 (1988).
21. J.B. Goodenough and A. Manthiram, Physica C 157, 439 (1989).
22. J.M. Tranquada, A.H. Moudden, A.I. Goldman, P. Zolliker, D.E. Cox, G. Shirane, S.K. Sinha, D. Vaknin, D.C. Johnston, M.S. Alvarez, A.J. Jacobson, J.T. Lewandowski, and J.M. Newsam, Phys. Rev. B 38, 2477 (1988).
23. R.J. Birgenau, D.R. Gabbe, H.P. Jensen, M.A. Kastner, P.J. Picone, T.R. Thurston, G. Shirane, Y. Endoh, M. Sato, K. Yamada, Y. Hidaka, M. Oda, Y. Enomoto, M. Suzuki, and T. Murakami, Phys. Rev. B 38, 6614 (1988).
24. J.M. Tranqnada, S.M. Heald, A.R. Moodenbaugh, and W.M. Temmerman, Phys. Rev. B 35, 1613 (1987); ibid. B36, 5263 (1987).
25. N. Nücker, J. Fink, J.C. Fuggle, P.J. Durham, and W.M. Temmerman, Phys. Rev. B 37, 5158 (1988).
26. Y. Dai, A. Manthiram, A. Campion, and J.B. Goodenough, Phys. Rev. B 38, 5091 (1988).
27. F.J. Himpsel, G.V. Chandreshakar, A.B. McLean, and M.W. Shafer, Phys. Rev. B 38, 11946 (1988).
28. J.B. Goodenough, J. Mater. Education. 9, 620 (1987).
29. P. Steiner, V. Kinsinger, I. Sander, B. Siegwart, S.Hüfner, C. Politis, R. Hoppe, and H.P. Müller, Z. Phys. B – Condensed Matter 67, 497 (1987).
30. K. Allan, A. Campion, J. Zhou and J.B. Goodenough, (unpublished).
31. H. Müller-Buschbaum and W. Wollschlager, Z. Anorg. Allg. Chem. 414, 76 (1975).
32. J. Gopalakrishnan, M.A. Subramanian, C.C. Torardi, J.P. Attfield, and A.W. Sleight, Mat. Res. Bull. 24, 321 (1989).
33. T. Tokura, H. Takagi, and S.Uchida, Nature 337, 345 (1989); H. Takagi, S.Uchida, and Y. Tokura, Phys. Rev. Lett. 62, 1197 (1989).
34. A. Manthiram, X.X. Tang, and J.B. Goodenough, Phys. Rev. B 37, 3734 (1988).
35. K. Takita, H. Akinaga, H. Katoh, H. Asano, and K. Masuda, Jpn. J. Appl. Phys. 27, L67 and L1676 (1988).
36. M.W. Shafer, T. Penney, B.L. Olson, R.L. Greene, and R.H. Koch, Phys. Rev. B 39, 2914 (1989).
37. Y.J. Uemura, V.J. Emery, A.R. Moodenbaugh, M. Suenaga, D.C. Johnston, A.J. Jacobson, J.T. Lewandowski, J.H. Brewer, R.F. Kiefl, S.R. Kreitzman, G.M. Luke, T. Riseman, C.E. Stronach, W.J. Kossler, J.R. Kempton, X.H. Yu, D. Opie, and H.E. Schone, Phys. Rev. B38, 909 (1988).
38. A. Manthiram and J.B. Goodenough, (unpublished).
39. Y. Tokura, J.B. Torrance, T.C. Huang, and A.I. Nazzal, Phys. Rev. B38, 7156 (1988).
40. J.B. Goodenough, Proc. High-T_c Superconductors '88 Workshop, U.S. Dept. of Commerce NBS, Gaithersburg, MD, Oct. 11-12 (1988) (in press).
41. C.J. Hou, Masters Thesis, Univ. of Texas at Austin (1989).

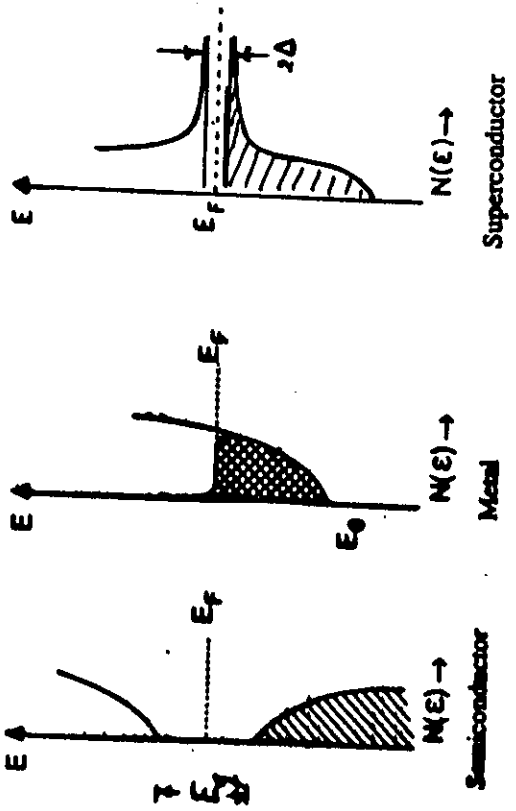

Determining Factors

1. Electronic, e.g. $N(E_F)$
2. Electron - Lattice coupling

ISOTOPE EFFECT

Definitions

Atomic mass numbers: $A = Z + N$

(Z = # of protons; N = # of neutrons)

Isotopes = nuclei of same Z, different N

Experiment:

$M^{\alpha} T_c = \text{const}$

for isotopes of a superconductor

BCS Theory

$$T_c \sim 1.14\ \Theta_D \exp(-1/\lambda)$$

$$\lambda = N(E_F)[V_C - V_{coul}];\quad \Theta_D \sim M^{-1/2}$$

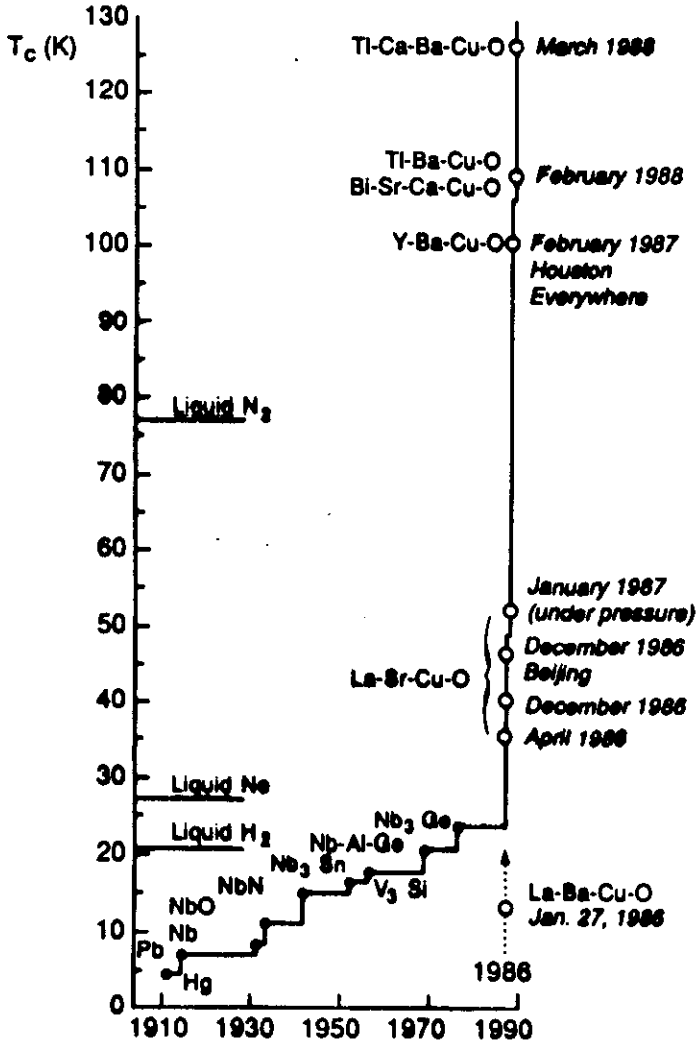
T_c (K)
130
120
110
100
90
80
70
60
50
40
30
20
10
0
1910
1930
1950
1970
1990
Tl-Ca-Ba-Cu-O
March 1988
Tl-Ba-Cu-O
Bi-Sr-Ca-Cu-O
February 1988
Y-Ba-Cu-O
February 1987
Houston
Everywhere
Liquid N_2
January 1987
(under pressure)
December 1986
Beijing
La-Sr-Cu-O
December 1986
April 1986
Liquid Ne
Liquid H_2
Nb_3 Ge
Nb-Al-Ge
Nb_3 Sn
V_3 Si
NbN
NbO
Nb
Pb
Hg
La-Ba-Cu-O
Jan. 27, 1986
1986

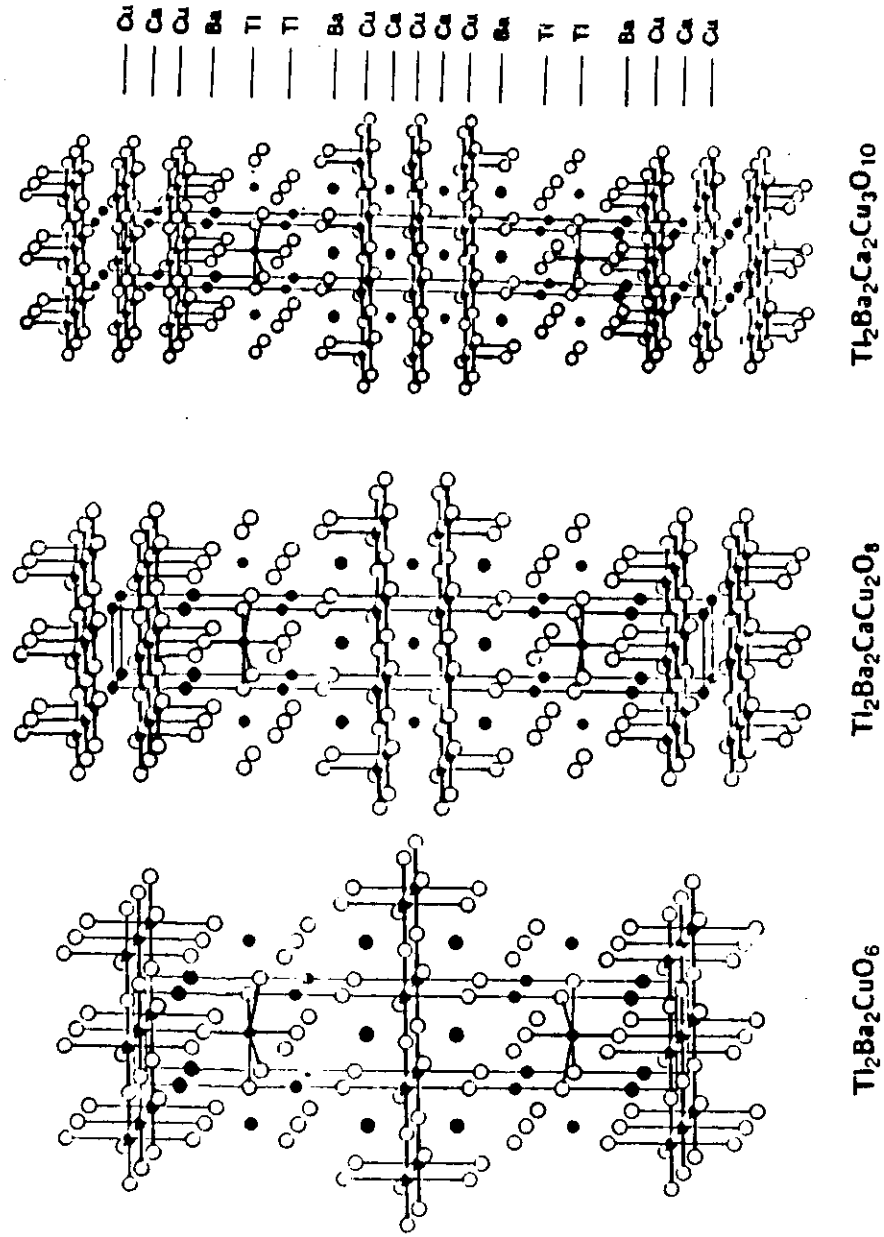
$Tl_2Ba_2Ca_2Cu_3O_{10}$
$Tl_2Ba_2CaCu_2O_8$
$Tl_2Ba_2CuO_6$

Figure 4.

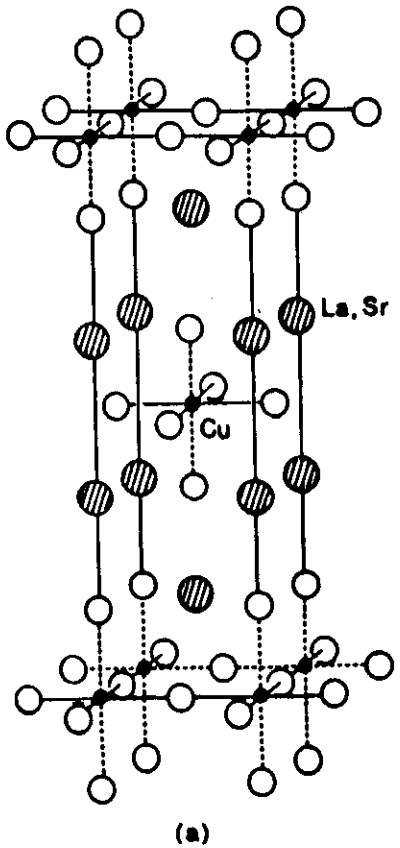

(a)

La_2CuO_4

Cu-O-Cu interactions

$\psi_{x2-y2} = N_\sigma (f_{x2-y2} - \lambda_\sigma \phi_\sigma - \lambda_s \phi_s)$

$b = (\psi_i H' \psi_j) = \varepsilon_{ij} N_\sigma^2 \lambda_\sigma^2$

$T_N \sim b^2/U \sim \lambda_\sigma^4/U$

$W = 2zb \sim \lambda_\sigma^2$

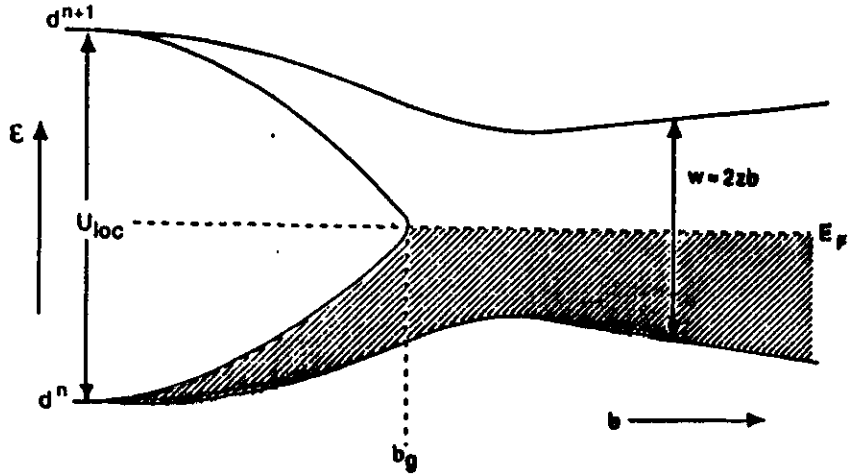

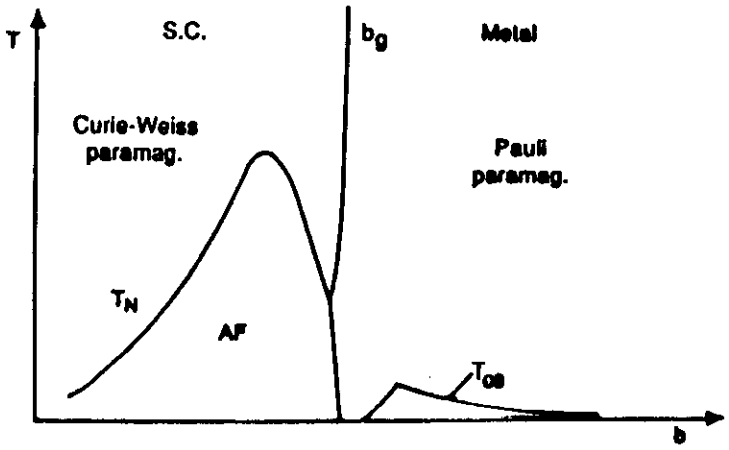

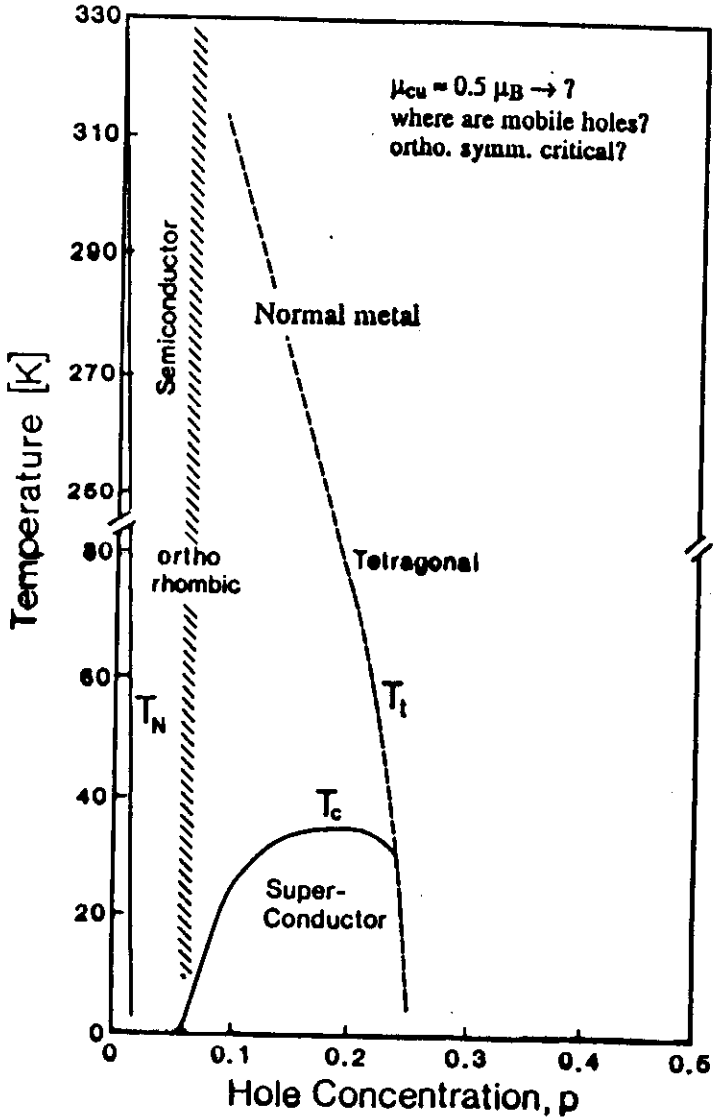

$La_{2-x}Sr_xCuO_y$

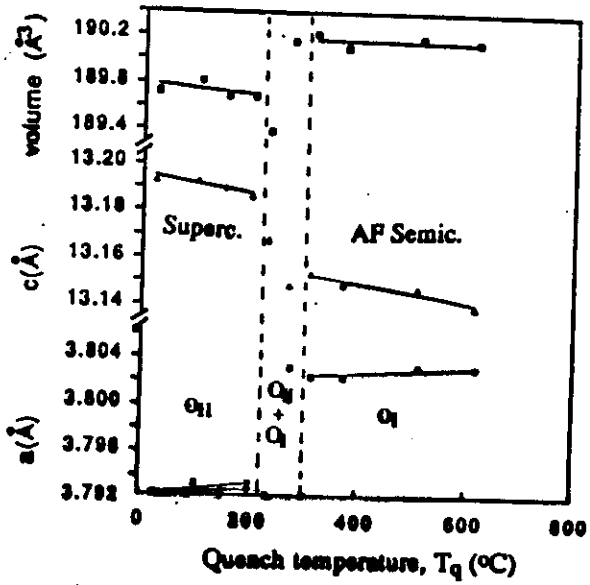

Heated in air from room T to T_q

$La_2CuO_{4+\delta}$ obtained at 800 °C and 23 kbar oxygen pressure

δ = 0.05 by iodometry

δ = 0.14 by TGA

J. Zhou

$La_2CuO_{4.05}$

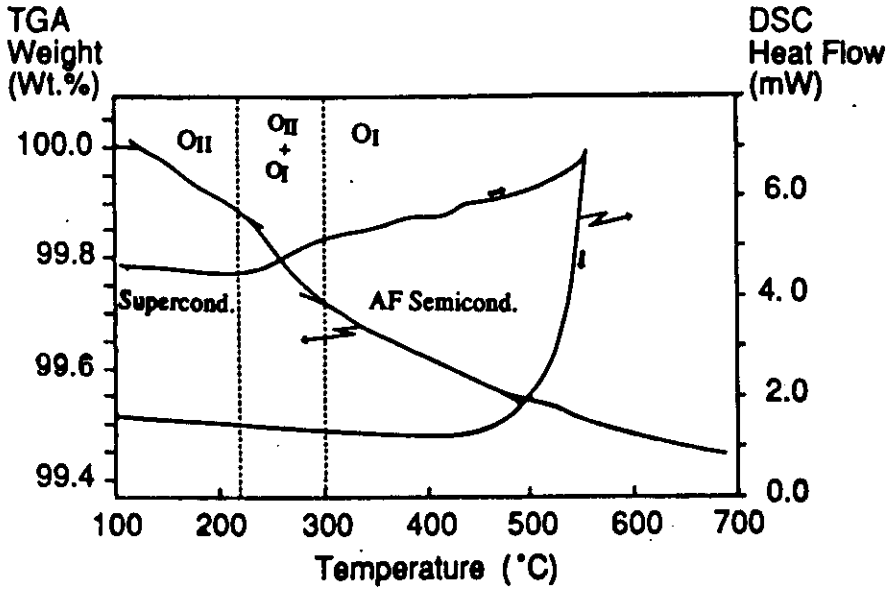

$La_{2-x}Sr_xCuO_{4-\delta}$

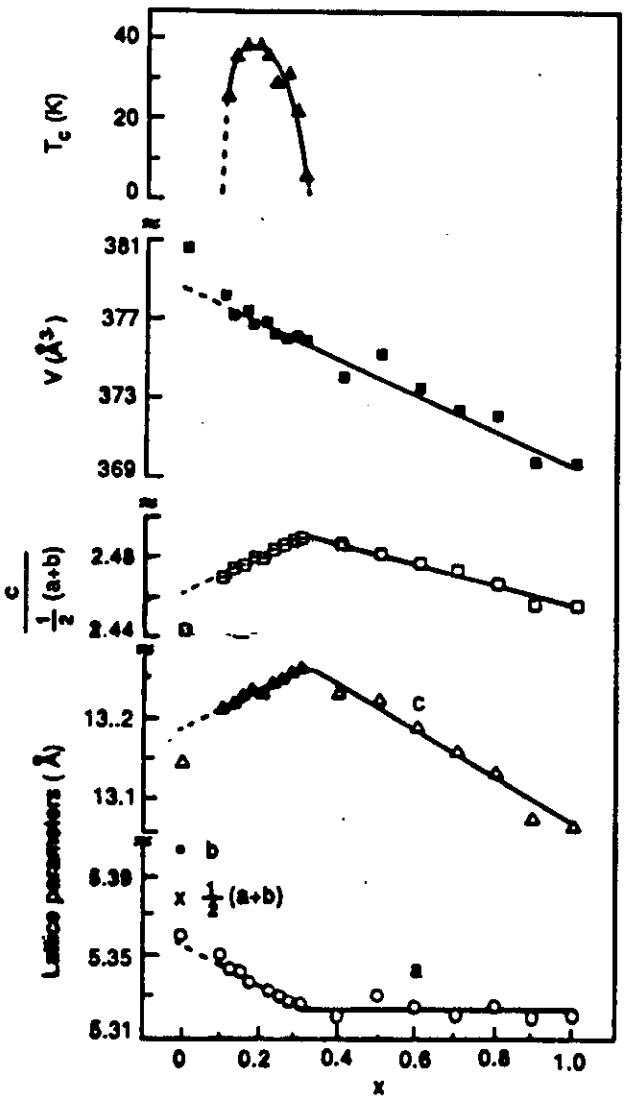

Tarascon et al

MgO

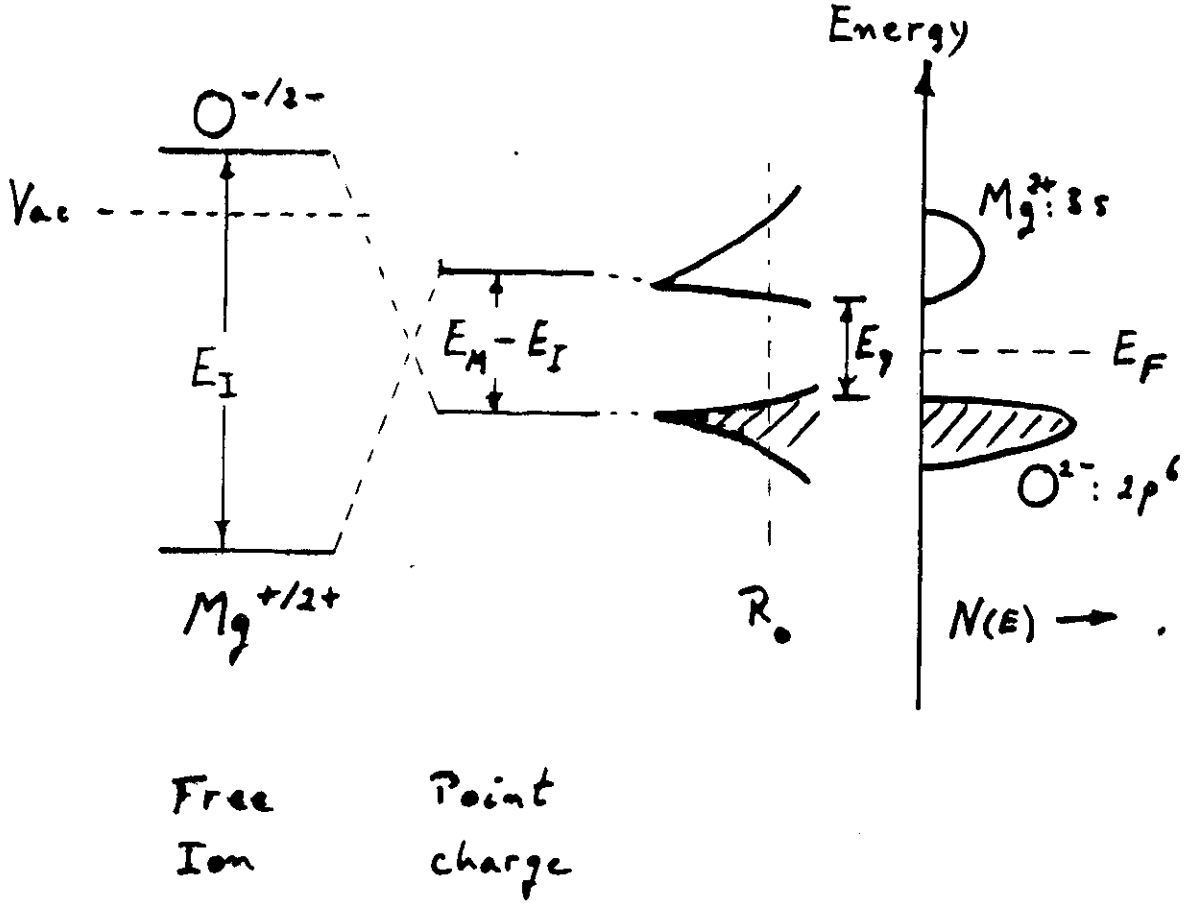

Free Ion

Point charge

MnO

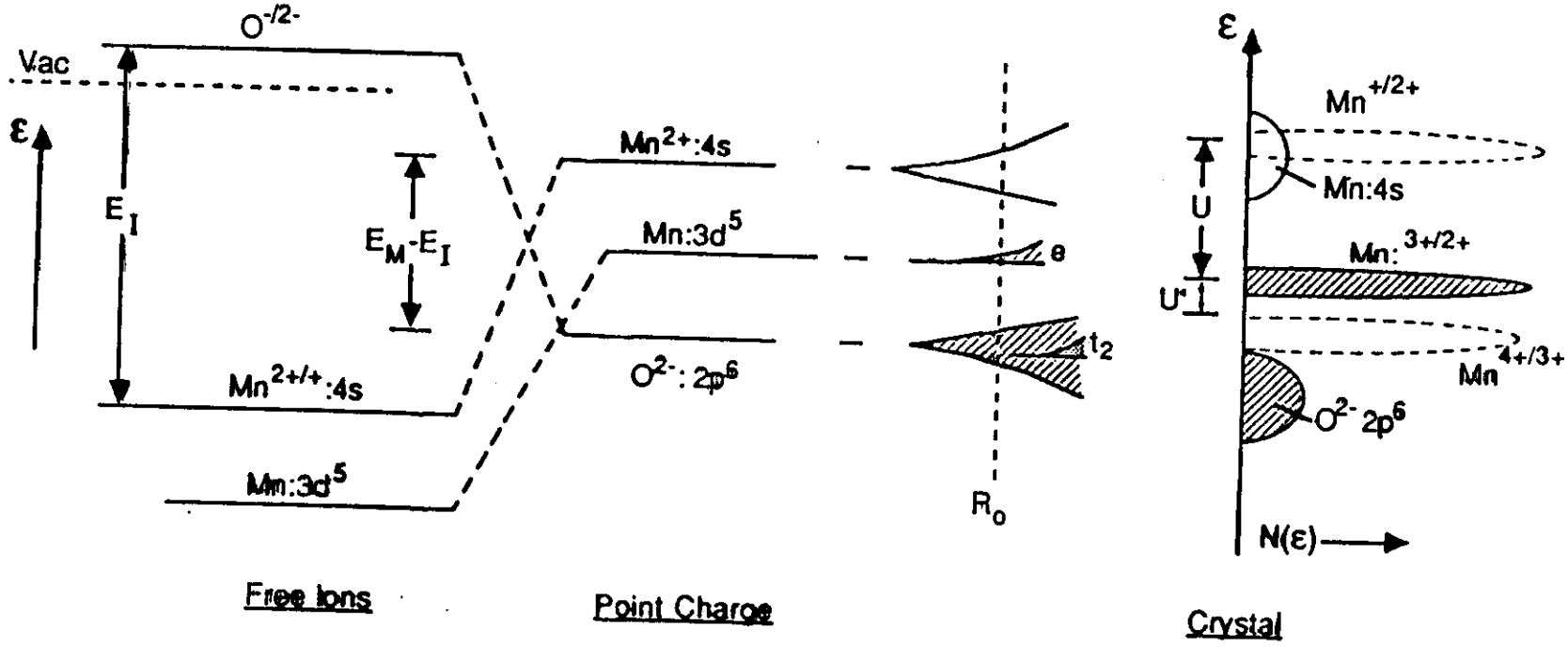
O-/2-
Vac
ε
E_I
E_M-E_I
Mn2+/+:4s
Mn:3d5
Mn2+:4s
Mn:3d5
O2-: 2p6
e
t2
R_o
ε
Mn+/2+
Mn:4s
U
U*
Mn: 3+/2+
Mn4+/3+
O2- 2p6
N(ε)
Free Ions
Point Charge
Crystal

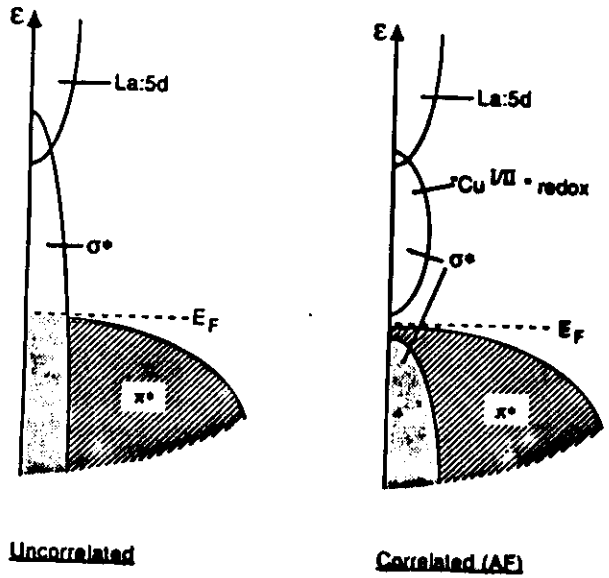

Uncorrelated

Correlated (AF)

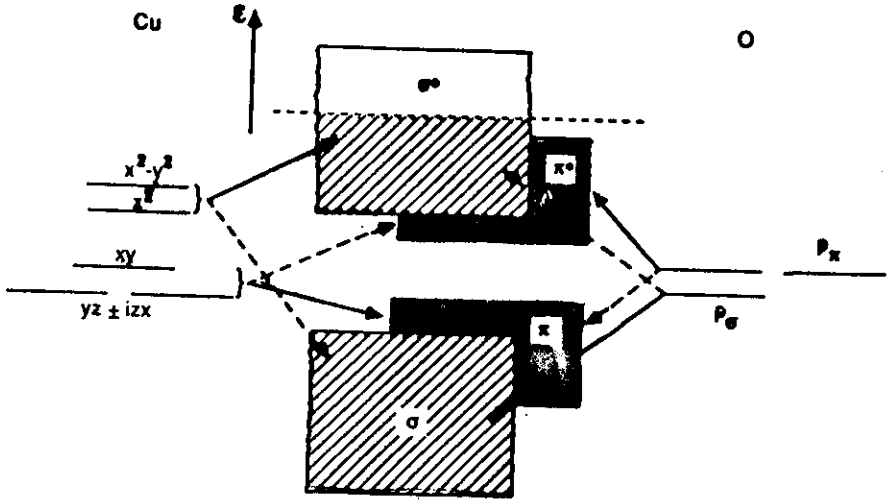

Origin of primarily O-2p character for π^*-band holes in superconductive state.

DENSITY OF ONE-ELECTRON STATES VS ENERGY FOR La_2CuO_4

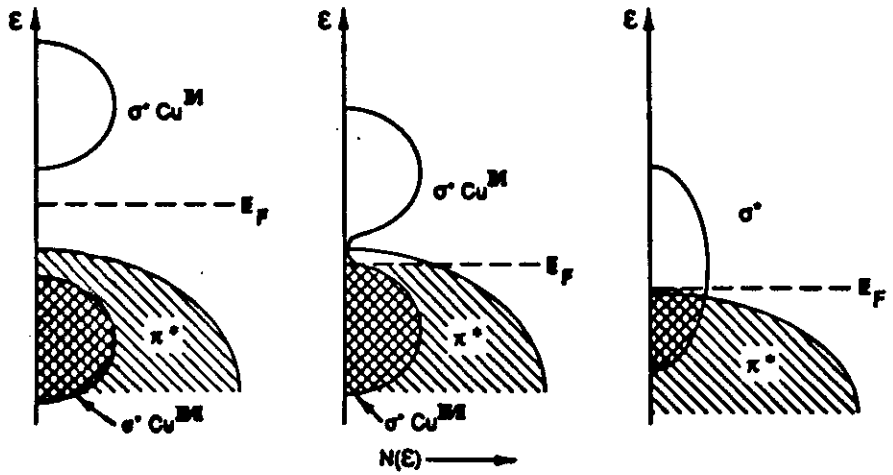

AF Semicond. Supercond. Normal metal

Cu-O-Cu angle < 180° Cu-O-Cu angle = 180°

$$t = \frac{(r_{La} + r_O)}{\sqrt{2}(r_{Cu} + r_O)}$$

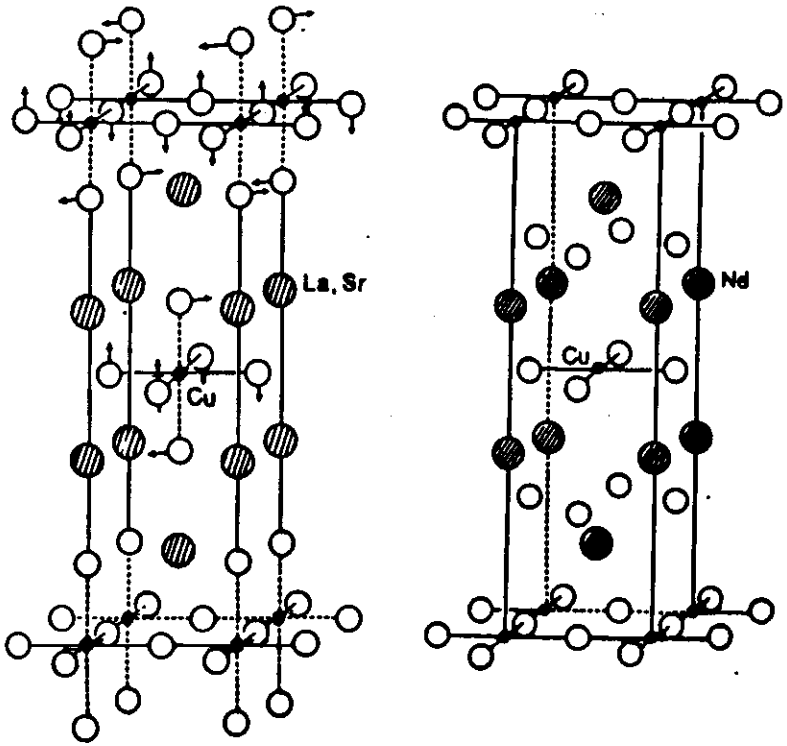

$La_{2-x}Sr_xCuO_4$ - p-type
Cu-O-Cu angle < 180°

$Nd_{2-x}Ce_xCuO_4$ - n-type
Cu-O-Cu angle = 180°

- Large polarizability
- Orbital hybridization adjusts readily to bond changes associated with lattice vibrations
- Strong electron-lattice coupling

Hybridization (or polarization) fluctuation mechanism

Takagi et al.